Molecular Crystals and Liquid Crystals

ISSN: 1542-1406 (Print) 1563-5287 (Online) Journal homepage: http://www.tandfonline.com/loi/gmcl20

Effects of Gold Nanorods on Photocurrents from Copper Phthalocyanine-Gold Nanorod Composite Films

Hiroaki Yonemura, Ippei Sakamoto & Sunao Yamada

To cite this article: Hiroaki Yonemura, Ippei Sakamoto & Sunao Yamada (2015) Effects of Gold Nanorods on Photocurrents from Copper Phthalocyanine-Gold Nanorod Composite Films, Molecular Crystals and Liquid Crystals, 620:1, 64-70, DOI: 10.1080/15421406.2015.1094864

To link to this article: http://dx.doi.org/10.1080/15421406.2015.1094864

Published online: 16 Dec 2015.

Mol. Cryst. Liq. Cryst., Vol. 620: pp. 64–70, 2015

ISSN: 1542-1406 print/1563-5287 online
DOI: 10.1080/15421406.2015.1094864

Taylor & Francis
Taylor & Francis Group

Effects of Gold Nanorods on Photocurrents from Copper Phthalocyanine-Gold Nanorod Composite Films

HIROAKI YONEMURA,[1,*] IPPEI SAKAMOTO,[2] AND SUNAO YAMADA[1]

[1]Department of Applied Chemistry, Faculty of Engineering, Kyushu University, Nishi-ku, Fukuoka, Japan
[2]Department of Materials Physics and Chemistry, Graduate School of Engineering, Kyushu University, Nishi-ku, Fukuoka, Japan

The fabrication of copper phthalocyanine (CuPc)–gold nanorod (AuNR) composite films on indium-tin-oxide electrodes was performed by electrostatic layer-by-layer adsorption technique. The photocurrents in CuPc–AuNR composite films were larger than those in CuPc films as a reference. The enhancements of the photocurrents in CuPc–AuNR composite films due to AuNR increased with increasing of wavelength up to near-infrared region. The enhancements are attributable to localized surface plasmon resonance (LSPR) due to AuNR. The enhancements at near-infrared wavelength due to the longitudinal LSPR were larger than those at visible wavelength due to the transverse LSPR.

Keywords gold nanorod; localized surface plasmon resonance; longitudinal mode; photocurrent; phthalocyanine; near-infrared

Introduction

Recently, photocurrent generation devices using organic compounds are expected to become the next generation of solar cells. However, most important issue is to improve the efficiency of photoelectric conversion. One of the methods for upgrading these devices is the use of localized surface plasmon resonance (LSPR) induced by the coupling of the incident electric field with the free electrons in the metal nanoparticles [1–11].

Previously, we reported the technique of electrostatic layer-by-layer adsorption for fabricating multistructures of silver nanoparticles (AgNPs) [3,7–10] and gold nanoparticles (AuNPs) [6, 11]. The technique is very convenient and needs no sophisticated equipment such as vacuum systems. Nevertheless, it is easy to control the deposition density of charged metal nanoparticles by the changing the immersion time of the substrate into the corresponding colloidal solution. Recently, we found the remarkable enhancement of

*Address correspondence to Hiroaki Yonemura, Department of Applied Chemistry, Faculty of Engineering, Kyushu University, 744 Motooka, Nishi-ku, Fukuoka 819-0395, Japan. E-mail: yonemura@mail.cstm.kyushu-u.ac.jp

Color versions of one or more of the figures in the article can be found online at www.tandfonline.com/gmcl.

photocurrent responses based on the photoexcitation of a tetraphenyl porphyrin, a zinc-tetraphenyl porphyrin, a palladium phthalocyanine derivative, or a poly(3-hexylthiophene) as an organic dye adsorbed onto the surfaces of AgNPs; the dye–AgNP assemblies were prepared by the layer-by-layer technique in the organic dye–AgNP composite films [3, 6–9]. Also, we found the remarkable enhancements of photocurrent responses in the composite films of a zinc-porphyrin-viologen linked compound as a donor–acceptor linked compound and AgNPs or AuNPs on ITO electrodes attributable to the combination of LSPR due to and photoinduced intramolecular electron-transfer [10, 11].

Gold nanorods (AuNRs) possess unique optical properties that are dependent on the size and the aspect ratio (AR: the ratio of the longitudinal-to-transverse length). A spherical AuNP has only one localized surface plasmon (SP) band in the visible region. By contrast, AuNRs have a couple of localized SP bands. One localized SP band corresponds to the transverse mode, which absorbs in the visible region around 520 nm. On the other hand, the other SP band corresponds to the longitudinal mode that absorbs in the far- to near-infrared region. The LSPR properties can be tuned via the AR of the AuNR [12]. The AuNRs have a high sensitivity to the dielectric constant of the surrounding medium (e.g. solvent, substrates, adsorbents and the inter-distances of AuNRs) [13–16]. Recently, we reported the effects of magnetic processing on the orientation and the organization of AuNR / poly(sodium 4-styrenesulfonate) (PSS) composites [17], AuNRs with three different ARs [l-AuNR (AR = 8.3), m-AuNR (AR = 5.0), and s-AuNR (AR = 2.5)] [18], or gold nanowires (AuNWs), which have AR up to 10 [19], on a substrate. However, effects of AuNRs on photocurrent of organic dye–AuNR composite films have not been elucidated yet.

In this study, we examined the effects of enhanced electric fields resulting from LSPR of AuNR (longitudinal and transverse modes) on the photocurrents of copper phthalocyanine (CuPc)–AuNR composite films.

Experimental

Poly(ethyleneimine) (PEI, Mw = 50,000 – 1100,000, Wako), poly(sodium 4-styrenesulfonate) (PSS, average Mw = ~70,000 Sigma-Aldrich), copper phthalocyanine-tetrasulfonic acid tetrasodium salt (CuPc, Sigma-Aldrich), tetrabutylammonium perchlorate (TBAP, TCI), ferrocene (Fc, TCI) and other chemicals were used as received. The AuNRs were supplied by Dai Nippon Toryo Co. Ltd. (Osaka, Japan) and Mitsubishi Materials Co. Ltd. (Tokyo, Japan). The average length and width of the AuNRs were 18.5 nm and 5.2 nm, respectively (AR = 3.6) as determined from transmission electron microscope (TEM) images. The AuNRs in aqueous solution contain an excess amount of hexadecyltrimethylammonium bromide (CTAB) as a stabilizing agent. Centrifugation (20,000 *g*) of the aqueous AuNRs solution for 30 min was carried out twice to remove the excess CTAB.

The AuNR-PSS composites were prepared on the basis of the electrostatic interaction between CTAB as a stabilizing agent on the AuNR and PSS as described below [17]. Following centrifugation of the AuNR solution an aqueous solution of PSS (2 mg/ml) and NaCl (0.6 mM) was added and this solution was sonicated. The formation of AuNR-PSS composites was confirmed by the red-shift of the SP band which corresponds to the longitudinal oscillation mode in the near-infrared region.

CuPc–AuNR composite films were fabricated using the previous method [3, 6–11]. First, an indium tin oxide (ITO) electrode (10 Ω/sq.) was immersed into an aqueous PEI

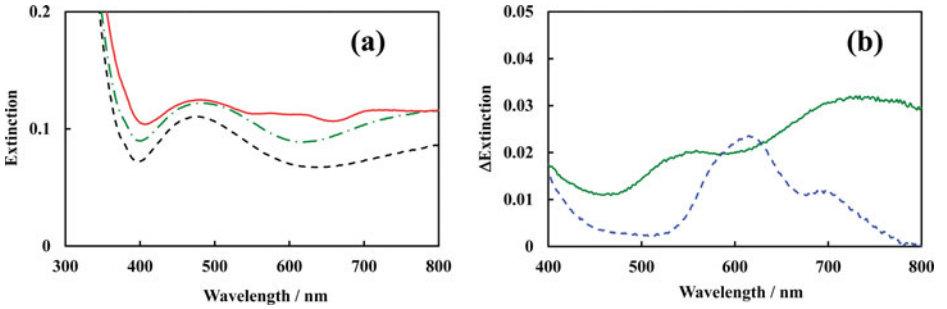

Figure 1. (a) Extinction spectra of CuPc/(AuNR-PSS/PEI)$_3$/ITO (red unbroken line), (AuNR-PSS/PEI)$_3$/ITO (green dash-dotted line), and PEI/ITO (black broken line). (b) Difference extinction spectra between (AuNR-PSS/PEI)$_3$/ITO and PEI/ITO (green unbroken line), and between CuPc/(AuNR-PSS/PEI)$_3$/ITO and (AuNR-PSS/PEI)$_3$/ITO (blue broken line).

solution (45 mg/ml) containing NaCl (0.2 M) for 20 min at 303 K to produce an ITO-electrode modified with PEI (PEI/ITO) (step 1). This positively charged ITO-electrode was then immersed into the aqueous colloidal solution of the negatively-charged AuNR-PSS composites for 6 hours to immobilize AuNR-PSS composites on the positively charged ITO-electrode by the electrostatic adsorption (AuNR-PSS/PEI/ITO) (step 2). By repeating step 1 and step 2 three times, multilayered films of AuNR-PSS and PEI, (AuNR-PSS/PEI)$_3$/ITO, were fabricated. Finally, 100 μl of a methanol solution of CuPc (0.5 mM) was spin-coated onto the surface of (AuNR-PSS/PEI)$_3$/ITO or PEI/ITO (CuPc/(AuNR-PSS/PEI)$_3$/ITO or CuPc/PEI/ITO) at 1000 rpm for 10 s and then 2000 rpm for 20 s by using photoresist spinner (KYOWARIKEN K-359S-1). Cyclic voltammetry (CV) and differential pulse voltammetry (DPV) were carried out in benzonitrile solution of CuPc containing 0.1 M tetrabutylammonium percholorate (TBAP) as a supporting electrolyte on an ALS 420 model EQCM instrument (BAS) using a three-electrode cell equipped with platinum working and counter electrodes, and an Ag wire as a reference electrode. The redox peak of ferrocenium/ferrocene ($Fc^{\bullet+}$/Fc) was used as an external standard. Before measurements, nitrogen bubbling was carried out for 30 min.

Photocurrent measurements were carried out with a 150W Xe lamp through a monochromator in acetonitrile solution containing 0.1 M TBAP as a supporting electrolyte using the three-electrode photoelectrochemical cell; the three electrodes were modified (working), Ag wire (reference), and platinum (counter) as reported in previous paper [3, 6–11, 20–25]. All photocurrents were measured with a potentiostat (Fuso HECS-315B) under a controlled potential at E = 0 V versus Ag^+/Ag under ambient atmosphere, similar to the previous studies [3, 6–11, 23–25].

Results and Discussion

The characterization of CuPc/(AuNR-PSS/PEI)$_3$/ITO was carried out by extinction spectral and SEM measurements. Figure 1(a) shows the extinction spectra of CuPc/(AuNR-PSS/PEI)$_3$/ITO, (AuNR-PSS/PEI)$_3$/ITO, and PEI/ITO. Figure 1(b) shows the difference extinction spectra between (AuNR-PSS/PEI)$_3$/ITO and PEI/ITO, and between CuPc/(AuNR-PSS/PEI)$_3$/ITO and (AuNR-PSS/PEI)$_3$/ITO. The difference extinction spectrum between (AuNR-PSS/PEI)$_3$/ITO and PEI/ITO indicates that the CuPc–AuNR composite films (CuPc/(AuNR-PSS/PEI)$_3$/ITO) have two SP bands of AuNR. The broad absorption band

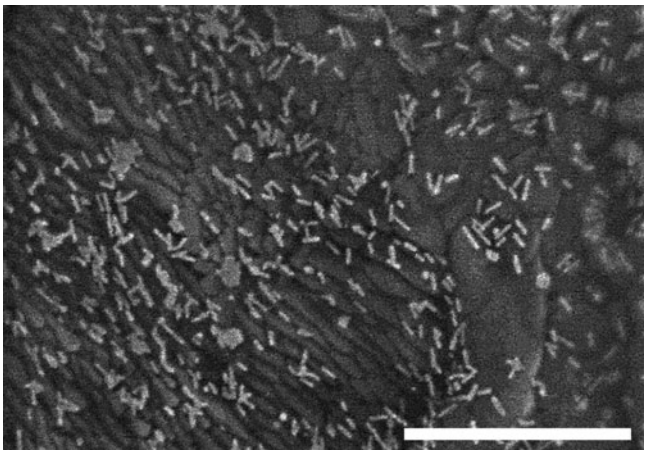

Figure 2. A SEM image of (AuNR-PSS/PEI)$_3$/ITO (scale bar = 300 nm).

at approximately 500−600 nm is assignable to the SP band due to transverse modes of isolated AuNRs and/or small amount of aggregation of AuNRs; moreover, the broad bands at approximately 600−800 nm are assignable to the SP bands due to longitudinal modes of isolated AuNRs and/or small amount of aggregation of AuNRs (Fig. 1), as reported previously [17, 18]. The results are in consistent of that there are a number of the isolated AuNRs and the aggregation of AuNRs were hardly observed in SEM image of (AuNR-PSS/PEI)$_3$/ITO (Fig. 2). The density of AuNRs was estimated to be 11% by SEM images of (AuNR-PSS/PEI)$_3$/ITO (Fig. 2). In addition, the difference extinction spectrum between CuPc/(AuNR-PSS/PEI)$_3$/ITO and (AuNR-PSS/PEI)$_3$/ITO indicates that CuPc/(AuNR-PSS/PEI)$_3$/ITO has broad absorption band (670–800 nm) due to CuPc. The absorption spectrum of the adsorbed CuPc (Fig. 1(b)) is in good agreement with that of CuPc methanol solution. The result strongly indicates no aggregation of CuPc on the surface of (AuNR-PSS/PEI)$_3$/ITO.

In CuPc–AuNR composite films and CuPc films, stable cathodic photocurrents were observed. The photocurrent action spectra of two samples (Fig. 3(a)) were in good agreement with the absorption spectrum of CuPc in methanol solution, in CuPc/PEI/ITO, or in

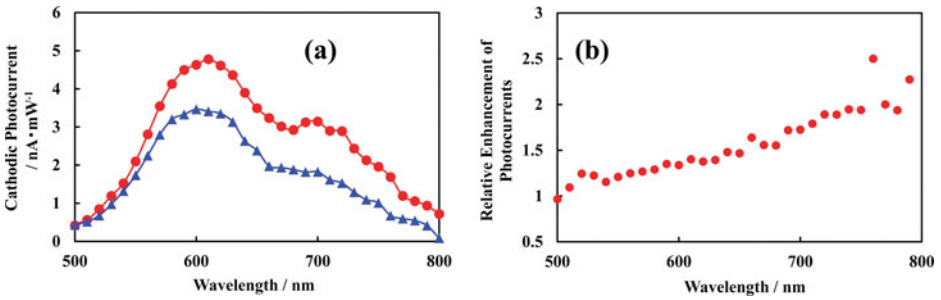

Figure 3. (a) Photocurrent action spectra of CuPc/PEI/ITO (▲) and CuPc/(AuNR-PSS/PEI)$_3$/ITO (●). (b) Relative enhancements of photocurrents of CuPc/(AuNR-PSS/PEI)$_3$/ITO as estimated by the photocurrent ratios of CuPc/(AuNR-PSS/PEI)$_3$/ITO to CuPc/PEI/ITO.

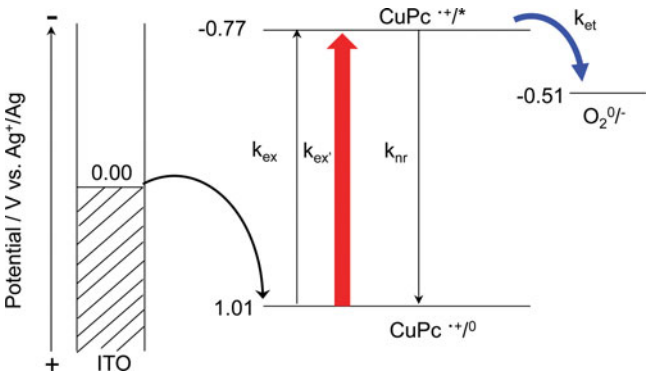

Figure 4. Schematic presentation of reaction scheme of photoelectrochemical reactions in CuPc/(AuNR-PSS/PEI)$_3$/ITO. k_{et} : rate constant of photoinduced electron-transfer from the excited state of CuPc (CuPc*) to O_2, k_{ex}: rate constant of excitation of CuPc, k_{ex}': rate constant of excitation of CuPc in the presence of AuNR (LSPR enhanced excitation), k_{nr} : rate constant of non-radiative process of CuPc*.

CuPc/(AuNR-PSS/PEI)$_3$/ITO (Fig. 1(b)). Therefore, it is suggested that the photocurrents are attributable to the photoexcitation of CuPc. The redox potentials of CuPc in benzonitrile were examined by CV and DPV measurements. From the CV and DPV results, the oxidation potential of CuPc was estimated to be 1.01 V vs Ag^+/Ag. On the basis of the observations, the photocurrents are attributable to the photoexcitation of CuPc and the subsequent photoinduced electron transfer from the excited state of CuPc (CuPc*) to oxygen in the electrolyte solution (Fig. 4).

It is noteworthy that the photocurrents in CuPc/(AuNR-PSS/PEI)$_3$/ITO were larger than those in CuPc/PEI/ITO (Fig. 3(a)). Furthermore, the relative enhancements of photocurrents increased with increasing of wavelength up to near-infrared region and the relative enhancements (1.5–2.5) at one Q band of CuPc in the longer wavelength (670–800 nm) were much larger than those (1.0–1.5) at the other Q band of CuPc in the shorter wavelength (520–670 nm) (Fig. 3(b)).

The large enhancement of surface-enhanced Raman scattering for the excitation of longitudinal SP band was observed as compared with that for the excitation of transverse SP band in the dye-AuNR conjugate in the previous paper [26]. The result is attributable to that the large enhancements of local electric field due to longitudinal SP band of AuNR are stronger than those due to transverse SP band of AuNR, because of the simulation of finite-difference time-domain. In the present study, since two bands due to the Q bands of CuPc overlap the transverse and the longitudinal SP bands of AuNR (Fig. 1(b)), the enhancements of photocurrent generation based on the immobilized CuPc are most likely to attributable to the local electric fields due to two SP bands of AuNR appearing in the vicinity of AuNR surface (LSPR enhanced excitation) (Fig. 4) [26–28]. The large portion of the Q band in the shorter wavelength (500–670 nm) overlaps the transverse SP band of AuNR, while the small portion of it overlaps the longitudinal SP band of AuNR (Fig. 1(b)). On the other hand, the Q band in the longer wavelength (670–800 nm) overlaps the only longitudinal SP bands of AuNR (Fig. 1(b)). Therefore, the large enhancements of photocurrents in the longer wavelength (670–800 nm) in Fig. 3 strongly suggest that the local electric fields due to longitudinal SP band of AuNR are stronger than those due to transverse SP band of AuNR [26–28].

Conclusions

The large enhancements of the photocurrents in CuPc–AuNR composite films were observed at near-infrared wavelength, as compared with those at visible wavelength. The results are most likely ascribed to stronger local electric fields of LSPR corresponding to the longitudinal mode of AuNR, as compared with those corresponding to the transverse mode of AuNR. Further investigations on the effects of AR and density of AuNRs on the photocurrents in CuPc–AuNR composite films are now in progress.

Acknowledgments

The authors thank the Center of Advanced Instrumental Analysis, Kyushu University for performing SEM and TEM measurements, respectively. The authors thank Dr. Daigou Mizoguchi (Dai Nippon Toryo Co. Ltd.) for providing the AuNRs. The present study was supported by Grants-in-Aid for Scientific Research (No. 25600006, No. 24651145), Nanotechnology Network Project (Kyushu-area Nanotechnology Platform), and Joint Usage/Research Program on Zero-Emission Energy Research, Institute of Advanced Energy, Kyoto University (ZE26A-27), from MEXT of Japan.

References

[1] Atwater, H. A. & Polman, A. (2010). *Nat. Mater.*, *9*, 205.
[2] Akiyama, T., Nakada, M., Terasaki, N., & Yamada, S. (2006). *Chem. Commun.*, 395.
[3] Arakawa, T., Munaoka, T., Akiyama, T., & Yamada, S. (2009). *J. Phys. Chem. C*, *113*, 11830.
[4] Sugawa, K., Akiyama, T., Kawazumi, H., & Yamada, S. (2009). *Langmuir*, *25*, 3887.
[5] Akiyama, T., Aiba, K., Hoashi, K., Wang, M., Sugawa, K., & Yamada, S. (2010). *Chem. Commun.*, *46*, 306.
[6] Takahashi, Y., Taura, S., Akiyama, T., & Yamada, S. (2012). *Langmuir*, *28*, 9155.
[7] You, J., Takahashi, Y., Yonemura, H., Akiyama, T., & Yamada, S. (2012). *Jpn. J. Appl. Phys.*, *51*, 02BK04.
[8] Matsumoto, R., Yonemura, H., & Yamada, S. (2013). *J. Phys. Chem. C*, *117*, 2486.
[9] Matsumoto, R., Yamada, S., & Yonemura, H. (2013). *Jpn. J. Appl. Phys.*, *52*, 04CK07.
[10] Matsumoto, R., Yamada, S., & Yonemura, H. (2013). *Mol. Cryst. Liq. Cryst.*, *579*, 243, 115.
[11] Matsumoto, R., Yamada, S., & Yonemura, H. (2014). *Mol. Cryst. Liq. Cryst.*, *598*, 86.
[12] Link, S., Wang, Z. L., & El-Sayed, M. A. (1999). *J. Phys. Chem. B*, *103*, 3073.
[13] Jain, P. K., Eustis, S., & El-Sayed, M. A. (2006). *J. Phys. Chem. B*, *110*, 18243.
[14] Nakashima, H., Furukawa, K., Kashimura, Y., & Torimitsu, K. (2007). *Chem. Commun.*, *10*, 1080.
[15] Nie, Z., Fava, D., Kumacheva, E., Zou, S., Walker, G. C., & Rubinstein, M. (2007). *Nat. Mater.*, *6*, 609.
[16] Nie, Z., Fava, D., Rubinstein, M., & Kumacheva, E. (2008). *J. Am. Chem. Soc. 130*, 3683.
[17] Yonemura, H., Suyama, J., Arakawa, T., & Yamada, S. (2009). *Thin Solid Films*, *518*, 799.
[18] Yonemura, H., Sakai, N., Suyama, J., & Yamada, S. (2011). *J. Photochem. Photobiol. A: Chem.*, *220*, 179.
[19] Yonemura, H., Makihara, Y., Sakai, N., Iwasaka, M., & Yamada, S. (2014). *Mol. Cryst. Liq. Cryst.*, *598*, in press.
[20] Yonemura, H., Tahara, H., Ohishi, K., Iida, S., & Yamada, S. (2010). *Jpn. J. Appl. Phys.*, *49*, 01AD04.
[21] Tahara, H., Yonemura, H., Harada, S., & Yamada, S. (2011). *Mol. Cryst. Liq. Cryst.*, *539*, 121.
[22] Tahara, H., Yonemura, H., Harada, S., & Yamada, S. (2011). *Jpn. J. Appl. Phys.*, *50*, 081605.
[23] Yonemura, H., Yuno, K., Takata, M., & Yamada, S. (2011). *Mol. Cryst. Liq. Cryst.*, *538*, 171.

[24] Yonemura, H., Takata, M., & Yamada, S. (2013). *Mol. Cryst. Liq. Cryst.*, *579*, 120.
[25] Yonemura, H., Takata, M., & Yamada, S. (2014). *Jpn. J. Appl. Phys.*, *53*, 01AD06.
[26] Gabudean, A. M., Focsan, M., & Astilean, S. (2012). *J. Phys. Chem. C*, *116*, 12240.
[27] Ming, T., Zhao, L., Yang, Z., Chen, H., Sun, L., Wang, J., & Yan, C. (2009). *Nano Lett.*, *9*, 3896.
[28] Su, H., Zhong, Y., Ming, T., Wang, J., & Wong, K. S. (2012). *J. Phys. Chem. C*, *116*, 9259.